Int. J. Solids Structures Vol. 17, pp. 707–715 1981.
Printed in Great Britain.

0020-7683/81/070707-08$02.00/0
Pergamon Press Ltd.

DYNAMIC THREE-POINT BENDING OF SHORT BEAMS STUDIED BY CAUSTICS

P. S. THEOCARIS and N. P. ANDRIANOPOULOS

Department of Theoretical and Applied Mechanics, The National Technical University of Athens, 5, K. Zographou Street, Zographou, Athens 624, Greece

(*Received* 4 *February* 1980; *in revised Form* 10 *September* 1980)

Abstract—The problem of short beams having edge cracks normal to their longitudinal boundaries and subjected to three-point dynamic bending was studied experimentally by the method of caustics.

The crack propagation velocity and the Mode—I stress intensity factor were evaluated during crack propagation and the corresponding curves versus time were plotted. The important role of stress waves produced at the crack tip and the mutual interference between crack and neutral axis were studied.

INTRODUCTION

It is known that once a crack starts propagating, rather complex fracture phenomena are observed, involving crack arrest and acceleration, crack skewing and branching and stress-wave generation. Under some conditions, however, a single crack will transverse a normal cross-section up to complete failure.

It is of interest to determine the crack velocity and stress intensity factor as functions of time, or equivalently as functions of the instantaneous crack length after fracture initiation.

For some reasons, which will be discussed later, the dynamic three-point bending shows a more sensitive behavior to the above-mentioned phenomena than the simple dynamic traction. On the other hand, three-point bending is of interest in its own right.

A photoelastic investigation of the dynamic three-point bending can be found in[1]. Also, Kolsky[2], Bodner[3], Dao and Herrmann[4] have studied the nature of stress waves produced during fracture in the case of long bars submitted to three-point bending. But the geometry of the long bars used in these cases was not suitable for the study of the interaction between stress waves and the stress field of the propagating crack. Namely, the important first waves reflected from the longitudinal boundary ahead of the crack returned to the crack tip in an early time after crack initiation and their influence to crack propagation was not easily recorded due to triggering delays. On the other hand, waves travelled along the large dimension of the bar return to fracture area a long time after fracture completion. Kalthoff *et al.*[5] studied the initial steps of crack propagation under bending using a pre-initiation triggering technique, but their main goal was the determination of the crack initiation conditions.

In the present paper the optical method of caustics [6, 7] was applied to investigate the crack behaviour and its interference with stress waves when a dynamic load is applied in a three-point bending mode.

The geometry of the specimens used was similar to that of[1] since, under this geometry, the travelling time of the waves is well compared to the fracture duration. A preliminary presentation of the results derived from the investigation was made by the first author in a recent meeting[8].

THE EXPERIMENTAL METHOD

The method of caustics was applied for the study of the dynamic crack propagation in beams submitted to three-point bending. According to this method a light beam was impinged on the specimen at the close vicinity of the crack tip and the transmitted rays through the thickness of the beam were received on a reference plane parallel to the specimen. These rays were strongly deviated due to the strong thickness and refractive index variations at the region close to the crack tip and they were concentrated along a strongly illuminated curve on the reference plane (*the caustic*).

The governing equations of the caustic on the reference plane were found previously[6] and are expressed by

$$x' = \lambda r_0\left(\cos\vartheta + \frac{2}{3}\cos\frac{3\vartheta}{2}\right)$$

$$y' = \lambda r_0\left(\sin\vartheta + \frac{2}{3}\sin\frac{3\vartheta}{2}\right) \tag{1}$$

with

$$r_0 = \left(\frac{3C}{2\lambda}\right)^{2/5}, \quad C = \frac{z_0 t c_t K_I}{\sqrt{(2\pi)}}, \quad \lambda = \frac{z_i}{z_0 + z_i}. \tag{2}$$

In these relations z_0 represents the distance between the specimen and the reference plane (Fig. 1), t is the thickness of the specimen, c_t is the stress-optical coefficient for transmitted light rays[9] z_i represents the distance between the reference plane and the focus of the light beam, which coincides with each lens of the camera and ϑ is the angular coordinate around the crack tip.

From eqn[1] by introducing $x' = 0$ (the origin of (x', y') coordinate system is at the tip of the crack with positive x' direction along the crack direction (see Ref.[10])) it can be concluded that the transverse diameter D_t of the caustic is related to the radius r_0 of the *initial curve* of the caustic (that is the curve on the specimen engendering the caustic on the reference plane) by

$$D_t = 3.16\lambda r_0. \tag{3}$$

From Eqs (2) and (3) it is concluded that the Mode—I stress intensity factor K_I is given by

$$K_I = \frac{1.671}{z_0 t c_t \lambda^{3/2}}\left(\frac{D_t}{3.16}\right)^{5/2}. \tag{4}$$

EXPERIMENTAL PROCEDURE

A series of specimens was machined out from PMMA (plexiglas) with dimensions $0.30 \times 0.075 \times 0.004\ m^3$.

An initial slit of length $a_0 = 0.005$, 0.010 and 0.015 m was made by using a disk cutter of thickness 0.0003 m. A silverpaint line was applied at a small distance, ahead of the root of the slit, to furnish the necessary triggering signal. So, the system of recording the crack propagation was initiated when a real crack was already formed.

The tests were executed in an impact testing machine (Fig. 2) with a semicylindrically notched hammer of weight 17.17 N, falling from a height of 0.19 m.

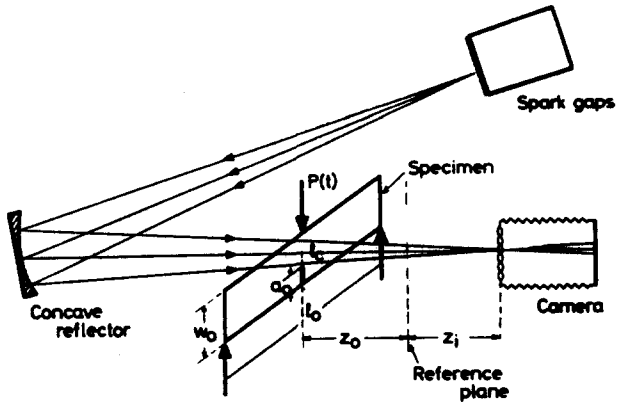

Fig. 1. Optical arrangement for transmitted caustics and specimen geometry.

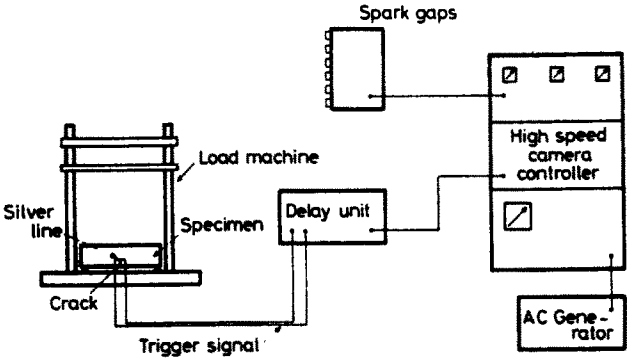

Fig. 2. Loading machine and experimental set-up.

A Cranz–Schardin high-speed camera has been used, with 24 spark-gap light-sources grouped together in a 6×4 array. Time intervals between spark-gap triggerings are indicated in the corresponding pictures.

In Fig. 3 transmitted caustics obtained during the fracture of a specimen, with initial crack length $a_0 = 0.01$ m are shown.

The crack-tip position was approximately defined by the center of the caustic. A spline interpolation method was used to derive the functions $v = v(a/w_0)$ and $K_I = K_I(a/w_0)$. This interpolation method was chosen, since it does not move the original points of the curve and so, the perturbations measured in the values of v and K_I remain unaffected. As it is known (see for example CONTROL DATA-BOEING "SCIENTIFIC ROUTINES PACKAGE") the spline interpolation method under some circumstances introduces a high frequency oscillation in the computed values of the function. This oscillation must be considered as an error since it could not be accepted as rational an oscillation with frequency equal to 0.1 or 0.01 of the frequency of the experimental data. Thus, the functions values obtained were smoothed once to eliminate this error and final forms are plotted in Figs. 4–6 for the three initial lengths used in the tests.

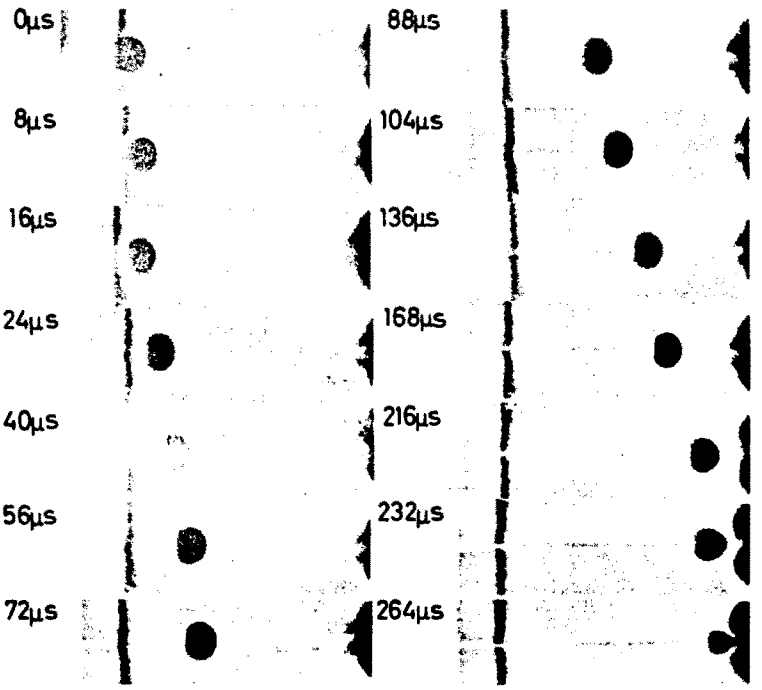

Fig. 3. Transmitted caustics in three-point bending. Initial crack length $a_0 = 0.01$ m.

RESULTS AND CONCLUSIONS

It can be immediately seen from Figs. 4 to 6 that there is:

(i) A strong fluctuation in the values of both velocity v and the stress intensity factor K_I.

(ii) A continuous falling of these values in the sense of the mean value.

(iii) A slight time-shift between v and K_I, with K_I laging v.

In order to present a reasonable explanation of the above described phenomena it is necessary to modify the basic assumption made in Ref.[11] that the crack runs into a constant stress field which unloads. This assumption must be changed by the assumption that the crack tip is facing a falling stress field, which becomes zero when the crack arrives at the boundary of the specimen.

Really, the driving stress of crack propagation is σ_x (normal to the crack), which is not constant along a cross section of the specimen, but changes sign from tensile at the side of the crack, to compressive at the side ahead the crack, being zero somewhere in the middle of the specimen. So, the value of σ_x at the crack-tip is a function of the distance between crack-tip and the point where $\sigma_x = 0$. Since this distance cannot be constant, as the crack propagates, it is evident that σ_x cannot be constant. The line produced by the points with $\sigma_x = 0$ of all the cross sections will be called in the sequel as the "*neutral axis*" of the specimen.

In order to define the position of the neutral axis it was necessary to run a series of photoelastic experiments with various initial crack lengths. The corresponding isochromatic fringe patterns for Araldite-B specimens are shown in Fig. 7. In these patterns a heavily dark point is always shown between the crack tip and the point of the load application. It is a zero order or neutral point where all the stresses are zero. So, it is a point belonging to the neutral axis. More points of the neutral axis cannot be obtained, since in all sections, except the middle one, the shear stress τ_{xy} is not zero.

Taking into consideration that the neutral axis is a continuous, smooth line, we can conclude that this axis passes somewhere through the mid-points between the first-order fringes above and below the neutral point.

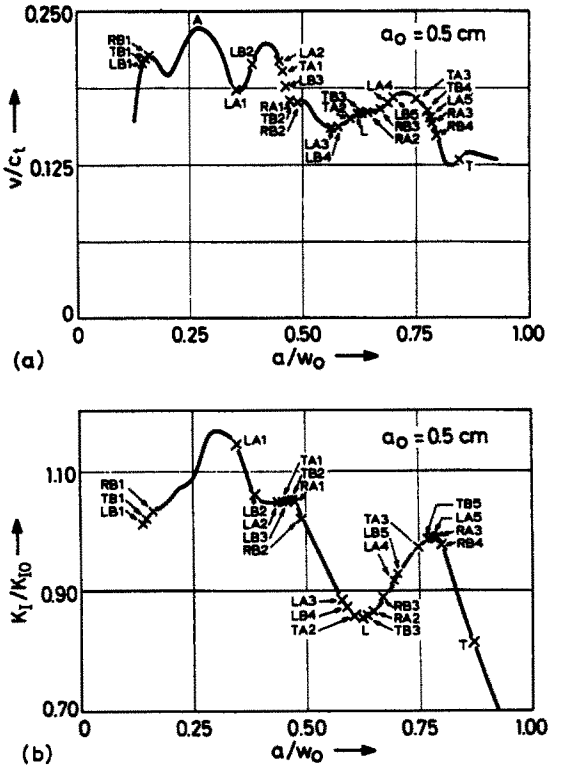

Fig. 4. Crack velocity (a) and stress intensity factor K_I (b) vs crack length for initial crack length $a_0 = 0.005$ m.

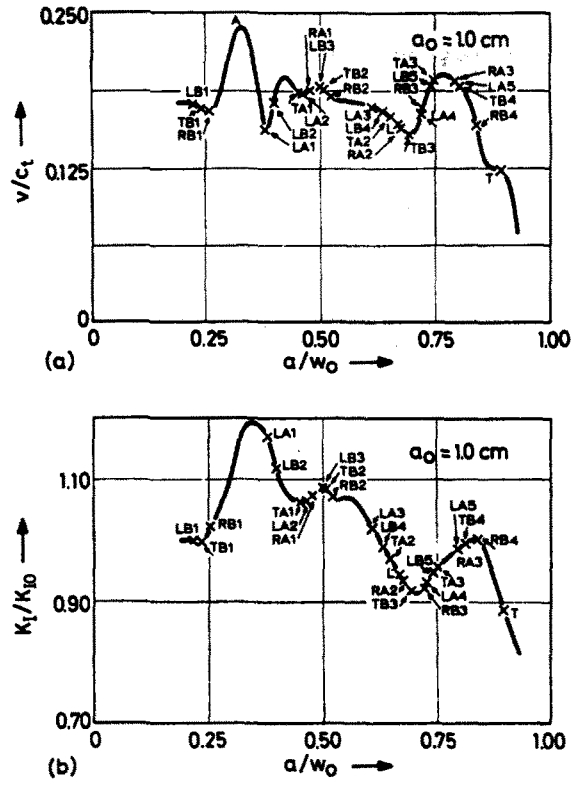

Fig. 5. Crack velocity (a) and stress intensity factor K_I (b) vs crack length for initial crack length $a_0 = 0.01$ m.

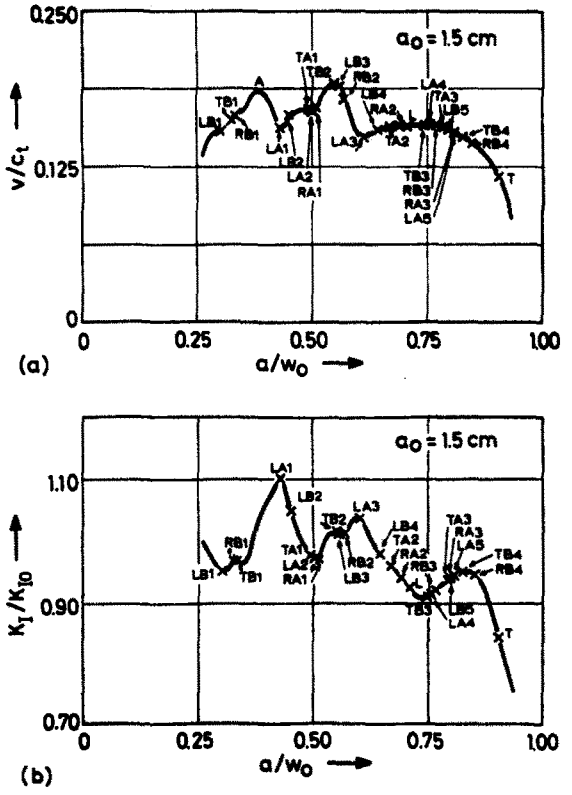

Fig. 6. Crack velocity (a) and stress intensity factor K_I (b) vs crack length for initial crack length $a_0 = 0.015$ m.

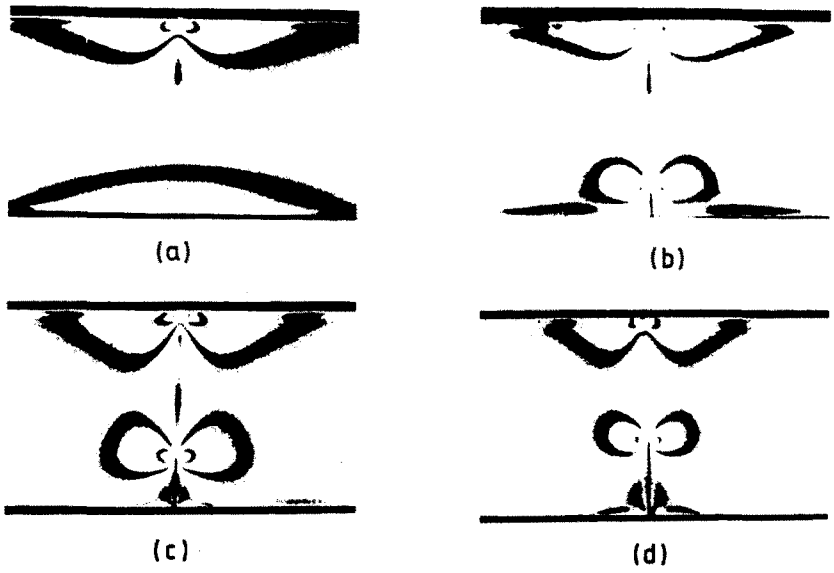

Fig. 7. Photoelastic pattern of the neutral axis. (Fig. 7(a) represents the uncracked specimen, 7b, c and d show slitted specimens with initial crack lengths $a_0 = 0.125\ w_0$, $0.250\ w_0$ and $0.375\ w_0$, where w_0 is the width of the strip.)

As we can see in Fig. 7(a), in the case of the uncracked specimen, the neutral point lies in the close vicinity of the point of the load application, i.e. the neutral axis passes near the load point. In Fig. 7(b), where the crack length is 0.125 of the specimen-width, the neutral point (and so the neutral axis) still remains in roughly the same position. When this reduced crack length equals 0.25 the neutral point has moved to the mid-place between crack tip and load point and when the reduced crack length becomes 0.375, this point goes just ahead the crack tip. So, when the reduced crack length equals about 1/3 (the mean value of 0.25 and 0.375) the neutral point is moving rapidly to the crack tip. Thus we can describe the behaviour of the neutral axis as follows:

(i) The neutral axis passes near the load point when the crack length is less than 1/3 of the specimen width.

(ii) The neutral axis moves to the crack tip area when the reduced crack length equals about 1/3.

(iii) The neutral axis remains in the vicinity of the crack tip for crack lengths greater than about 1/3.

This assumption of the combined movement of the neutral axis of the beam with the propagating crack-tip justifies the continuous falling of the values of v and K_I in the sense of the mean value and does not imply the necessity to accept some kind of "inertial" behaviour of the neutral axis, as it was suggested in Ref.[1]. This behaviour could mislead into unacceptable conclusions such as the tip of the propagating crack may enter compressive regions of the beam.

Also, the fact that the crack tip is always moving in an extension region can be definitely concluded from the continuous existence of the caustic of the type indicating an extensive area of stress around the crack tip. It is well-known that, in compression, natural cracks do not produce caustics and slits form cusped caustics.

On the other hand, the curved crack path (Fig. 8), may be justified by the assumption that small random inequalities in the extension stress of the two regions, left and right of the crack, may produce balancing shear stresses, which result in a divergence of the crack.

It is well-known that, when a crack propagates, stress waves are produced at the crack tip by the fracture phenomenon. The waves are spatial, longitudinal and transverse, waves and surface Rayleigh waves with velocities $c_L = 2{,}170$ m/sec, $c_T = 1{,}410$ m/sec and $c_R = 1{,}360$ m/sec respectively. These waves are reflected at the longitudinal boundaries of the specimen.

Fig. 8. Crack path with initial crack length $a_0 = 0.015$ m.

Taking into consideration that the whole fracture process lasts about 250 μsec, the transverse and Rayleigh waves can run along the width of the beam more than four times, while the longitudinal stress waves more than seven times. Obviously, after two or three reflections the direct influence of these waves may be ignored due to their attenuation and dispersion involved, but this does not mean that there are not secondary effects such as, stationary waves.

Nevertheless, stress waves, created in a previous time by the crack tip and passing later through it, change the stress field. This change depends on the amplitude and the phase of each wave.

A full theoretical analysis of the interference between crack and crack-produced waves is very complicated as the apparent analogy between this phenomenon and the electronic feedback case is misleading. Feedback can be described by a small number of well-defined parameters and laws, while a corresponding set in fracture would be rather complicated.

In our case, we try to find some indications postulating the existence of such an interference between crack characteristics (velocity, stress intensity factor) and stress waves. We define the points on the crack path at which the wave fronts, produced at time $\tau = 0$, meet the crack tip, having previously reflected at the specimen boundaries. Having in mind Fig. 1 we can write eqn (5) for a wave front once reflected at the boundary ahead of the crack as:

$$l_c = \int_0^{\tau} v(\tau)\,\mathrm{d}\tau = 2(w_0 - a_0) - c_i, \quad i = L, T, R. \tag{5}$$

This integral equation was solved numerically and the length l_c was obtained. Relative equations hold for waves having their first reflection at the transversal boundary of the specimen ahead or behind the crack.

We introduce the following notation: L, T or R: Longitudinal, Transversal or Rayleigh waves. A or B: First reflection Ahead or Behind the crack. 1, 2, 3...: Total number of reflections.

We can now establish the Table 1, in which the values of $a = a_0 + l_c$, for each type of wave, are computed for the three values of a_0 referred previously. The values of Table 1 have been marked as discrete points along the curves of Figs. 4–6.

Although it is hard to say that these points give a unique answer to problem, it is out of any doubt that in all cases the arrival of LA1-wave (Long ahead, once reflected) is followed by a rapid increase of velocity and a respective decrease of K_I.

In addition, the almost simultaneous arrival of LB1-TB1- and RB1-waves is followed by a decrease of either velocity, or acceleration (for $a_0 = 0.015$ m) without a significant influence in the value of K_I.

The arrival of LB2-wave produces a delayed decrease of velocity, which was increased by the LA1-wave.

The higher-order reflections do not seem to influence strongly the crack characteristics. Single letters L or T denote the arrival points of the longitudinal and transversal waves reflected at the transversal (the shortest ones) boundaries of the specimen. These waves seem to have no influence on the crack-propagation behavior.

Finally, there is no wave contribution in the creation of the maximum, pointed by the letter A in the curves of velocity of the respective figures. The existence of this maximum could be justified by the mutual interference between the crack tip and the neutral axis.

From the photographs of Fig. 7 we can see that, when the crack length equals about the

Table 1. The reduced crack-length a/w_0 of the wave-front for three different initial crack-lengths, used in the tests.

a_0 m 10^{-2} / a/w_0	0.5	1.0	1.5
LA1	.353	.378	.417
LA2	.447	.467	.501
LA3	.566	.591	.611
LA4	.689	.717	.734
LA5	.775	.794	.796
LB1	.147	.222	.302
LB2	.382	.400	.450
LB3	.462	.502	.556
LB4	.582	.618	.638
LB5	.706	.748	.784
TA1	.454	.460	.486
TA2	.607	.620	.656
TA3	.741	.752	.766
TB1	.160	.244	.330
TB2	.472	.506	.548
TB3	.634	.692	.732
TB4	.766	.810	.824
RA1	.469	.481	.501
RA2	.644	.677	.689
RA3	.781	.800	.797
RB1	.163	.256	.337
RB2	.491	.524	.568
RB3	.675	.727	.771
RB4	.799	.843	.851

one-third of the specimen-width, the neutral axis turns its notch from the load side to the crack-tip side. This fact results in a rather strong decrease of the stress field around the crack tip, with a consequent decrease in crack velocity and the stress intensity factor.

Beyond this point, as we have already mentioned, the neutral axis precedes the crack tip by a constant distance.

Another observation is that in the final stage, the crack diverges significantly from a straight line (Fig. 8), and either meets the boundary by an angle different to a right-angle, or, while following an almost semicircular path, meets the boundary by an angle roughly equal to 90° (as it was observed in Ref.[1]). A possible explanation of this phenomenon is that the hammer, after its fall, relays on the boundary producing a static compressive field. The crack is forced to avoid this field by changing its direction of propagation. However, a close examination of the specimens after fracture did not show any correlation between the direction of divergence and the small asymmetries in either the support of the specimens or their loading.

Relatively to the observed time-shift between v and K_I, with K_I laging v, this lag was also reported in[1] and it is somehow surprising since in simple tension experiments K_I precedes v. But, this time-shift (as in bending) was also observed in the case when a crack approaches an interface[12]. In our case as a local interface may be considered the neutral axis because along

this axis a change in sign for the normal stresses takes place. This relative behavior of K_I and v does not allow the establishment of any kind of linear relation between them, except, perhaps, at the initial-acceleration phase.

A closing question arises now. Why the same phenomena do not appear in a simple tension experiment? The answer lies on the experimental[13] and theoretical[14] fact that a cracked tension specimen needs a much higher load to fracture than the load corresponding to fracture of a specimen under a three-point bending. Thus, the influence of the stress waves in the latter case is much more significant than in the case of fracture under tensile loading. Crack propagation velocity is, also, lesser in the case of three-point bending compared with the corresponding quantity in the case of simple tension.

The above described sensitive behaviour of a crack in three-point bending implies that it is preferable to use this loading mode than the tensile mode in order to study the interference between cracks and stress waves.

This sensitivity can be explained if one considers that the critical stress needed to initiate crack propagation (which is roughly the same for both tensile and bending loads) can be achieved in the bending mode with an external load almost to one half of the corresponding load in the tensile mode, due to unequal stress-distribution in the first of the modes. But, after crack initiation, stress decreases rapidly in bending, as the crack comes closer and closer to the neutral axis, while in the tensile mode remains constant. Thus, the crack in bending propagates in a weak stress field, which allows the appearance of the abovementioned phenomena.

REFERENCES

1. A. S. Kobayashi and C. F. Chan, A dynamic photoelastic analysis of dynamic-tear-test specimen. *Exp. Mech.* **16**, 176–181 (1976).
2. H. Kolsky and D. Rader, Stress waves and fracture. *Fracture* (Edited by H. Liebowitz), Vol. 1. Academic Press, New York (1969).
3. S. R. Bodner, Stress waves due to fracture of glass in bending. *J. Mech. Phys. Solids* **21**, 1–8 (1973).
4. K. Dao and G. Herrmann, An experimental study of crack propagation in beams during fracture in bending. *Fracture Mechanics and Technology* (Edited by G. C. Sih and C. L. Chow), Vol. 11. Noordhoff (1977).
5. J. F. Kalthoff, S. Winkler and J. Beinert, The influence of dynamic effects in impact testing. *Int. J. Fracture* **13**, 528–531 (1977).
6. P. Manogg, Anwendung der Schattenoptik zur Untersuchung des Zerreisvorgangs von Platten. Dissertation 4/64, Universitaet Freiburg (1964).
7. P. S. Theocaris, Local yielding around a crack tip in plexiglas. *J. Appl. Mech.* **37**, *Trans ASME* **92**, Series E, 409–415 (1970).
8. P. S. Theocaris, Deeply cracked strips subjected to dynamic three-point bending by caustics, *Proc.* (*Zbormic*) 18*th Csek. Conf. Exp. Strain Analysis*, (Edited by T. Tavornicky), 1980.
9. D. D. Raftopoulos, D. Karapanos and P. S. Theocaris, Static and dynamic mechanical and optical behaviour of high polymers. *J. Physics D* (*Applied Physics*) **9** 869–877 (1976).
10. P. S. Theocaris, The reflected shadow method for the study of constrained zones in cracked birefrigent media. *J. Strain Analysis* **7**(2), 75–83 (1972).
11. J. Miklowitz, Elastic waves created during tensile fracture. *J. Appl. Mech* **20**, 122–130 (1953).
12. P. S. Theocaris and J. Milios, Crack-arrest at a bimaterial interface. *Int. J. Solids Structures.* **17**, 217–230 (1981).
13. F. Katsamanis, D. Raftopoulos and P. S. Theocaris, The dependence of crack velocity on the critical stress in fracture. *Exp. Mech.* **17**, 128–132 (1977).
14. B. C. O. E. Uwadiegwu, Single-edge cracked strip under three-point load. *Int. J. Engng Sci.* **15**, 413–420 (1977).